

UC Irvine

UC Irvine Previously Published Works

Title

Integrating Source Apportionment Tracers into a Bottom-up Inventory of Methane Emissions in the Barnett Shale Hydraulic Fracturing Region.

Permalink

<https://escholarship.org/uc/item/012846xg>

Journal

Environmental science & technology, 49(13)

ISSN

0013-936X

Authors

Townsend-Small, Amy
Marrero, Josette E
Lyon, David R
et al.

Publication Date

2015-07-01

DOI

10.1021/acs.est.5b00057

Copyright Information

This work is made available under the terms of a Creative Commons Attribution License, available at <https://creativecommons.org/licenses/by/4.0/>

Peer reviewed



Integrating Source Apportionment Tracers into a Bottom-up Inventory of Methane Emissions in the Barnett Shale Hydraulic Fracturing Region

Amy Townsend-Small,^{*,†} Josette E. Marrero,[‡] David R. Lyon,[§] Isobel J. Simpson,[‡] Simone Meinardi,[‡] and Donald R. Blake[‡]

[†]University of Cincinnati, Departments of Geology and Geography, Cincinnati, Ohio 45221, United States

[‡]University of California, Irvine, Department of Chemistry, Irvine, California 92697, United States

[§]Environmental Defense Fund, 301 Congress Ave., Suite 1300, Austin, Texas 78701, United States

Supporting Information

ABSTRACT: A growing dependence on natural gas for energy may exacerbate emissions of the greenhouse gas methane (CH_4). Identifying fingerprints of these emissions is critical to our understanding of potential impacts. Here, we compare stable isotopic and alkane ratio tracers of natural gas, agricultural, and urban CH_4 sources in the Barnett Shale hydraulic fracturing region near Fort Worth, Texas. Thermogenic and biogenic sources were compositionally distinct, and emissions from oil wells were enriched in alkanes and isotopically depleted relative to natural gas wells. Emissions from natural gas production varied in $\delta^{13}\text{C}$ and alkane ratio composition, with $\delta\text{D}-\text{CH}_4$ representing the most consistent tracer of natural gas sources. We integrated our data into a bottom-up inventory of CH_4 for the region, resulting in an inventory of ethane (C_2H_6) sources for comparison to top-down estimates of CH_4 and C_2H_6 emissions. Methane emissions in the Barnett are a complex mixture of urban, agricultural, and fossil fuel sources, which makes source apportionment challenging. For example, spatial heterogeneity in gas composition and high $\text{C}_2\text{H}_6/\text{CH}_4$ ratios in emissions from conventional oil production add uncertainty to top-down models of source apportionment. Future top-down studies may benefit from the addition of $\delta\text{D}-\text{CH}_4$ to distinguish thermogenic and biogenic sources.



■ INTRODUCTION

Methane (CH_4) is a greenhouse gas with a global warming potential 34 to 86 times greater than carbon dioxide (CO_2) on time scales of 100 and 20 years, respectively.¹ Production, processing, transmission, and distribution of natural gas, which is comprised primarily of CH_4 , are, along with agriculture and landfills, among the largest anthropogenic sources of CH_4 globally,^{2–4} nationally,^{5,6} and regionally.^{7,8} Natural gas combustion produces less CO_2 per unit of energy than coal or petroleum products; it has abundant domestic reserves, and its combustion releases less sulfur, nitrogen, and mercury than coal.^{9,10} However, among other potential negative impacts, a larger reliance on natural gas for electricity generation and transportation may increase CH_4 emissions, potentially overwhelming the climate benefit of natural gas.^{9,11} Measurements of fugitive emissions of CH_4 from along the natural gas supply chain are a critical first step in minimizing this problem.^{12–14}

Because of the large number of anthropogenic and natural sources of CH_4 , it can be difficult to assess the relative contribution of natural gas sources to CH_4 emissions. Uncertainties in activity factors and emissions factors can lead to underestimation of CH_4 emission rates using bottom-up approaches regionally,^{15,16} nationally,¹⁷ and globally.¹¹ Charac-

terization of stable isotopic^{7,18} and alkane ratio^{19,20} source signatures can help constrain CH_4 emissions from oil and gas sources,²¹ particularly in conjunction with top-down measurements of regional emission rates.^{22–24}

Here, we present measurements of $\delta^{13}\text{C}$, δD , and C_2-C_5 alkane ratios for CH_4 sources in the Barnett Shale natural gas producing region in northeast Texas. This region has tens of thousands of hydraulically fractured shale gas wells that can be sources of atmospheric CH_4 .²⁵ Produced gas (78–97% CH_4) is transported by a system of pipelines and gathering compressor stations to processing plants, which remove heavier hydrocarbons to create pipeline quality gas (~95% CH_4). This gas is transported through transmission pipelines and compressor stations to end users, including local industrial, commercial, and residential consumers. Older conventional oil wells in the region can also contribute CH_4 to the atmosphere.²¹ Finally, the Fort Worth–Barnett region is part of the United States' fourth largest metropolitan area, and there are urban CH_4

Received: January 6, 2015

Revised: April 8, 2015

Accepted: May 28, 2015

Published: July 7, 2015



sources including landfills, wastewater treatment plants, and power plants, as well as agricultural CH_4 sources including cattle ranches and feedlots. Our overall goals were (1) to characterize the isotopic and alkane ratios of CH_4 sources in the Barnett–Fort Worth region and (2) to integrate these data into a bottom-up CH_4 inventory for the region for comparison to top-down studies.

MATERIALS AND METHODS

Sample Collection. Whole air samples ($n = 119$) were collected in 2 L stainless steel canisters in October 2013 near Fort Worth, Texas during the Barnett Coordinated Campaign.²⁶ Most samples were collected downwind of CH_4 sources, including cattle feedlots, landfills, natural gas wells, and conventional oil wells (Figure 1). Five out of 119 samples

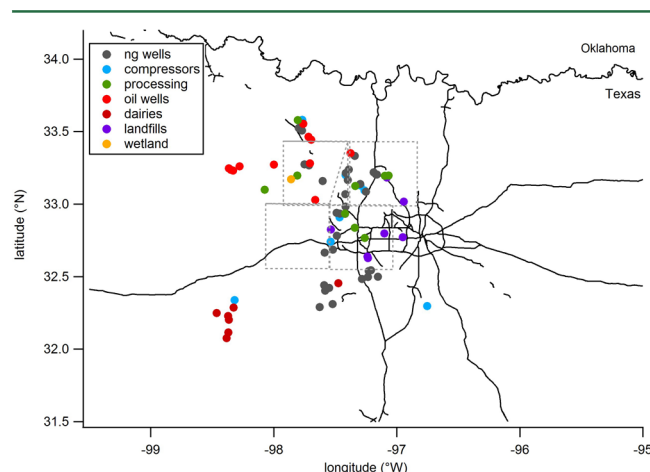


Figure 1. Map of sampling locations in the Barnett Shale–Fort Worth region. ng = natural gas. Dotted lines are the “core” Barnett Shale counties.

were collected directly at gas distribution and compressor station sources. We took 25 samples of background air upwind of the region. Location, time, type, and composition of all samples can be found in the Supporting Information. Prior to sampling, canisters were heated to 150 °C and then evacuated to 10^{-2} Torr.²⁷ Detailed canister preparation procedures have been described previously.²⁷ Sampling was guided by a Picarro Instruments G2301 $\text{CO}_2/\text{CH}_4/\text{H}_2\text{O}$ analyzer powered by the vehicle alternator.²⁸ This instrument was used to detect CH_4 enhancement only: canisters were not filled from the instrument exhaust or inlet. Canisters for source analysis were filled where CH_4 was elevated by at least 50 ppb, the minimum enhancement needed to detect isotopic source signatures.⁷ All samples were collected at ambient pressure by opening the canister valve for 60 s above and upwind of the sampling technician’s head.

Sample Analysis. The whole-air samples were analyzed at the University of California, Irvine via flame ionization detector (FID) for concentrations of CH_4 , ethane (C_2H_6 ; or C_2), propane (C_3H_8 ; C_3), n -butane ($n\text{-C}_4\text{H}_{10}$; C_4), and n -pentane ($n\text{-C}_5\text{H}_{12}$; C_5).²⁹ The CH_4 precision was 0.1% with an accuracy of 1%. The detection limit for $\text{C}_2\text{--C}_5$ alkanes was 3 parts per trillion by volume (pptv). The analytical precision ranged from 1% to 3%, and the accuracy was 5% (% relative standard deviation). Standards are traceable to NIST and subject to frequent intercalibration.²⁷

Subsamples of each canister were transferred to evacuated 12 mL glass vials (Exetainers, Labco Ltd., Buckinghamshire, UK) for analysis of $\delta^{13}\text{C}$ and δD of CH_4 via isotope ratio mass spectrometry at the University of Cincinnati.³⁰ The instrument was calibrated with CH_4 standards matched to sample concentrations to eliminate any possible linearity problems. The reproducibility of $\delta^{13}\text{C}$ and δD measurements using this method is 0.2‰ and 4‰, respectively,³⁰ and daily analysis of multiple replicates of CH_4 standards met or exceeded this.

Data Analysis. As gas concentrations for each sample type varied significantly, we used Keeling plots, where the isotopic ratio is regressed against $1/[\text{CH}_4]$ for each sample type and the y-intercept is the composition of excess CH_4 in the data set (Figures 2 and 3; Table 1).^{31–33} Concentrations of C_2H_6 ,

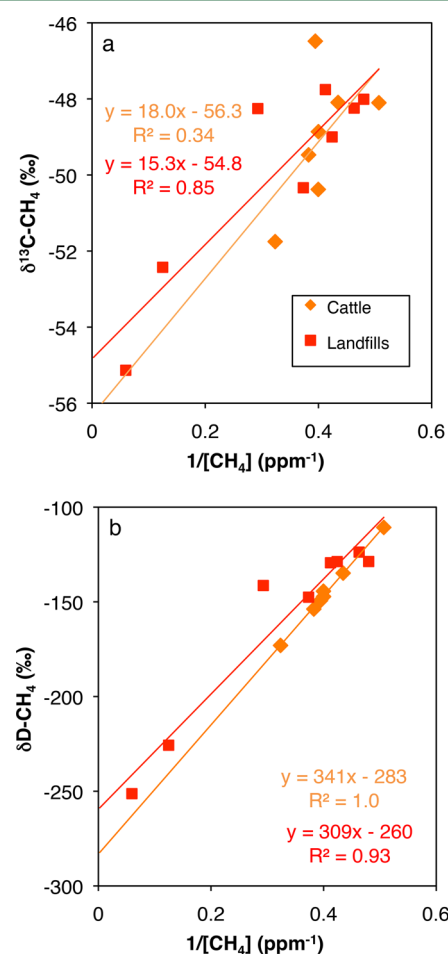


Figure 2. Keeling plots of (a) $\delta^{13}\text{C}\text{-CH}_4$ and (b) $\delta\text{D}\text{-CH}_4$ of biological methane sources sampled in the Barnett Shale region.

C_3H_8 , $n\text{-C}_4\text{H}_{10}$, and $n\text{-C}_5\text{H}_{12}$ were plotted against the concentration of CH_4 for each source type, such that the slope gives the average ratio of each alkane to CH_4 (Figures 3 and 4; Table 2).¹⁹ Isotope and alkane ratios for natural gas production sites were calculated by correcting for background air because our samples were taken downwind of production sites (Tables 3 and 4). For $\delta^{13}\text{C}$ and δD of CH_4 from individual samples, this correction was done according to ref 7 using the background air composition described below. For alkane ratios, we subtracted the background concentration of each alkane from the concentration measured in each source sample and then calculated the ratio of each $\text{C}_2\text{--C}_5$ alkane to CH_4 . Both

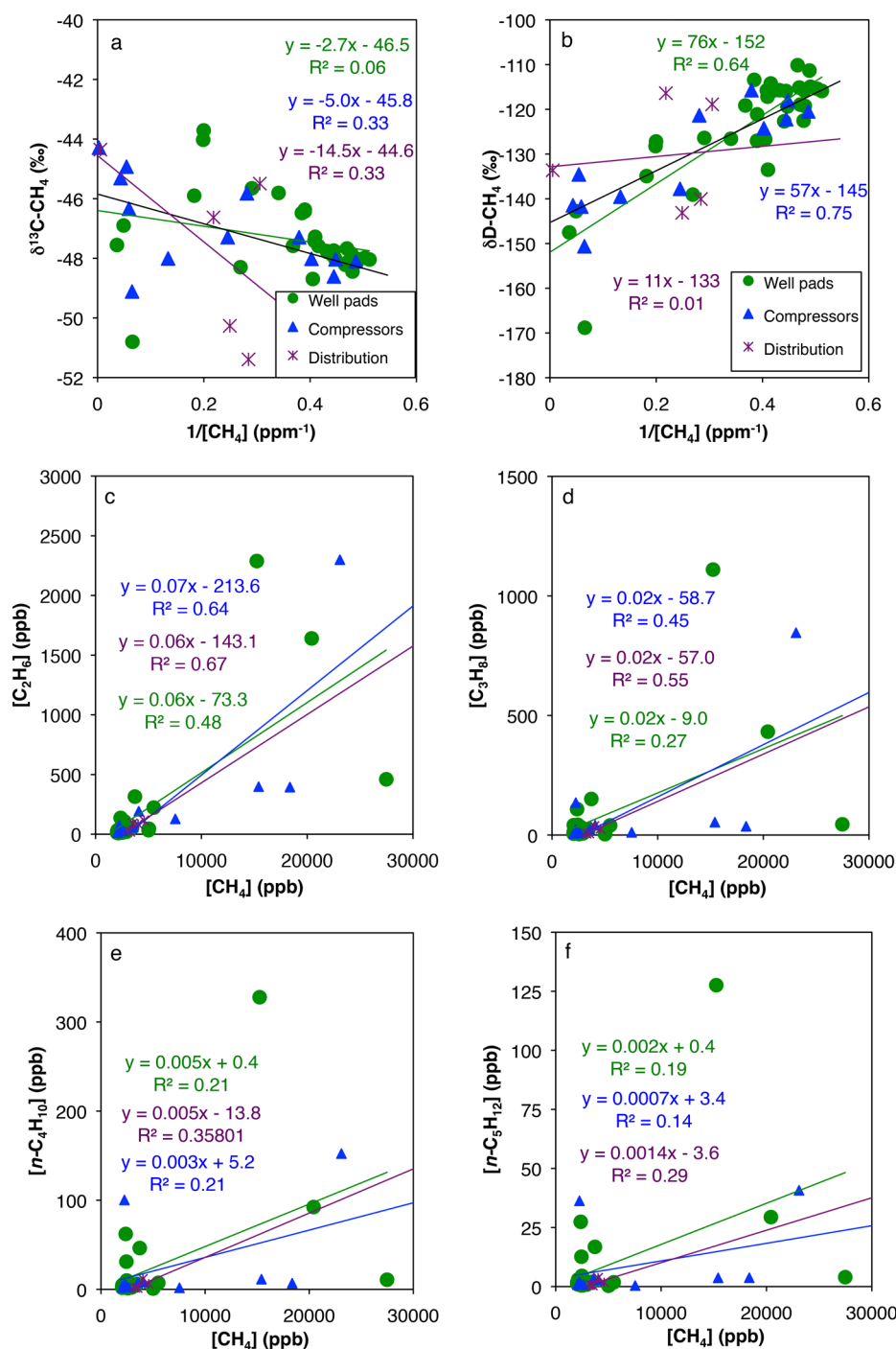


Figure 3. Composition of methane from natural gas sources in the Barnett Shale region. (a) Keeling plot of $\delta^{13}\text{C}-\text{CH}_4$ vs $1/[\text{CH}_4]$; (b) $\delta\text{D}-\text{CH}_4$ vs $1/[\text{CH}_4]$; (c) $[\text{C}_2\text{H}_6]$ vs $[\text{CH}_4]$; (d) $[\text{C}_3\text{H}_8]$ vs $[\text{CH}_4]$; (e) $[n\text{-C}_4\text{H}_{10}]$ vs $[\text{CH}_4]$; and (f) $[n\text{-C}_5\text{H}_{12}]$ vs $[\text{CH}_4]$.

Table 1. Stable Isotopic Endmembers for CH_4 Sources in the Barnett Shale Region^a

sample type	δD			$\delta^{13}\text{C}$		
	<i>n</i>	source endmember (‰)	<i>p</i>	<i>n</i>	source endmember (‰)	<i>p</i>
cattle	7	−283	<0.0001	7	−56.3	0.17
landfills	8	−260	0.0001	8	−54.8	0.001
natural gas well pads	35	−152	0.03	34	−46.5	0.14
transmission compressor stations	11	−145	0.0006	12	−45.8	0.05
distribution systems	5	−133	nd	5	−44.6	nd
conventional oil wells	7	−170	0.0001	4	−49.2	nd

^aData are derived from Keeling plots shown in Figures 2–4. *p* could not be determined (nd) for *n* < 6.

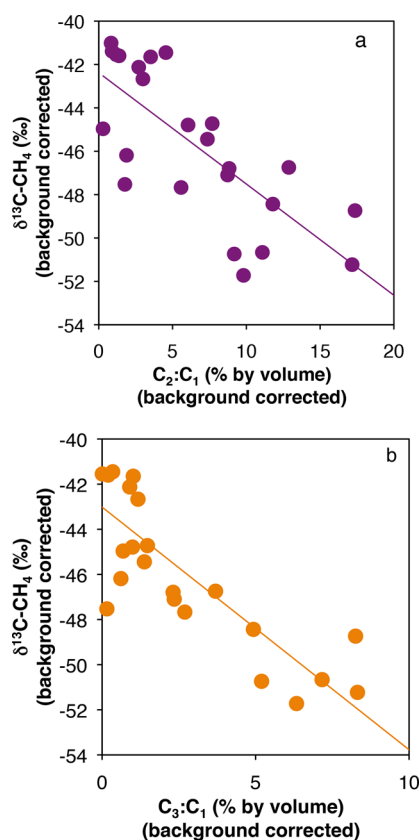


Figure 4. Relationship of $\delta^{13}\text{C}-\text{CH}_4$ with (a) C_2/C_1 and with (b) C_3/C_1 in samples taken from natural gas well pads, showing more isotopic depletion with increasing gas wetness.

the ratio plot and background correction techniques result in alkane ratios by volume, identical to the molar ratio.

RESULTS

Background air collected upwind of the region had an average (\pm SD) CH_4 concentration of 1.95 ± 0.07 ppm, a $\delta^{13}\text{C}$ value of -47.9 ± 0.2 ‰, and a δD of -114 ± 5 ‰. In October 2013, the average CH_4 concentration at Mauna Loa, Hawaii was 1.84 ± 0.01 ppm, with a $\delta^{13}\text{C}$ measured in October 2011 (the most recent year available) of -47.3 ‰.^{34,35} The lower CH_4 concentration in Hawaii (19° N) is partly due to its lower latitude relative to Fort Worth (33° N). The average concentration of C_2H_6 in background air near the Barnett during the campaign was 8.6 ± 3.7 ppb, as compared to 0.3–0.8 ppb measured in clean air in western California in September 2012 (D. Blake, personal communication). Background concentrations of C_3 , $n\text{-C}_4$, and $n\text{-C}_5$ alkanes were $5.0 \pm$

2.5, 1.8 ± 1.0 , and 0.6 ± 0.3 ppb, respectively (Supporting Information).

As expected, biological CH_4 sources were depleted in both D and ^{13}C with respect to thermogenic sources (Table 1, Figure 2).^{7,36,37} There was no relationship between CH_4 emitted from biological sources and concentration of other alkanes. Background-corrected values for the average isotopic signature of CH_4 emitted from biological sources (Table 3) are higher than the Keeling-plot derived endmembers (Table 1), because the Keeling plot method gives more weight to samples enriched in CH_4 with less contribution of background air to the observed isotopic signature.

Natural gas wells emitted CH_4 with δD and $\delta^{13}\text{C}$ signatures of -152 ‰ and -46.5 ‰, respectively (Table 1, Figure 3), although there was a weak relationship between $[\text{CH}_4]$ and $\delta^{13}\text{C}$ in well pad emissions (Table 1). $\delta^{13}\text{C}-\text{CH}_4$ decreased with increasing content of C_2H_6 and C_3H_8 at natural gas production sites (Figure 4). Ratios of background corrected C_2/C_1 in individual samples collected downwind of natural gas well pads ranged from 0.3% to 30.7%, and background-corrected $\delta^{13}\text{C}-\text{CH}_4$ ranged from -41.0 ‰ to -51.7 ‰. Other natural gas sources (compressor stations and local distribution systems) had similar isotopic and alkane ratio signatures to those observed at natural gas wells (Table 1, Figure 3). Natural gas from all sources was 6–7% C_2H_6 and $\sim 2\%$ C_3H_8 (Table 2, Figure 3). In general, concentrations of C_4 and C_5 alkanes were less than 1% of the CH_4 concentration (Table 2, Figure 3).

Conventional oil wells emitted CH_4 that was depleted in both ^{13}C and D relative to natural gas (Table 1). Emissions from conventional oil wells were enriched in $\text{C}_2\text{--C}_5$ relative to CH_4 as compared to natural gas sources (Table 2).

DISCUSSION

Tracers of CH_4 Emissions from Natural Gas Production. In general, for samples taken downwind of natural gas production sites, there was a poor correlation of $\delta^{13}\text{C}$ with CH_4 concentration (Table 1) and a wide range of ratios of $\text{C}_2\text{--C}_5$ alkanes to CH_4 (Figure 3). $\delta^{13}\text{C}-\text{CH}_4$ decreased with increasing concentrations of C_2 and C_3 alkanes at natural gas production sites in the Barnett region (Figure 4), as observed previously, due to varying degrees of thermal maturation of shale gas in the Barnett.³⁸ This high variability in gas composition at production sites throughout the region complicates the use of a single source apportionment indicator for attribution of regional CH_4 fluxes to natural gas production.

Our background-corrected C_2/C_1 data are compared with previous studies that have found a wide range of gas composition at natural gas production sites in the Barnett region, including regions of both wet and dry gas (Table 4, Figure 5).^{38,39} Our data have a higher average C_2/C_1 ratio than the other two studies, although we have a smaller number of

Table 2. Molar Ratios of $\text{C}_2\text{--C}_5$ Hydrocarbons to CH_4 (C_1) in Thermogenic CH_4 Sources in the Barnett Shale Region, as well as p Values Derived From Correlations in Figures 3 and 4^a

sample type	<i>n</i>	C_2/C_1 ratio	<i>p</i>	C_3/C_1	<i>p</i>	$n\text{-C}_4/\text{C}_1$	<i>p</i>	$n\text{-C}_5/\text{C}_1$	<i>p</i>
natural gas well pads	31	0.06	<0.0001	0.02	0.003	0.005	0.01	0.002	0.016
transmission compressor stations	10	0.07	0.006	0.02	0.03	0.003	0.2	0.0007	0.3
distribution systems	4	0.06	nd	0.02	nd	0.005	nd	0.001	nd
conventional oil wells	12	0.13	<0.0001	0.06	0.0003	0.02	0.001	0.006	<0.0001

^aBiological CH_4 sources are not shown; there was no relationship between alkanes and CH_4 in these sources. *p* could not be determined (nd) for $n < 6$.

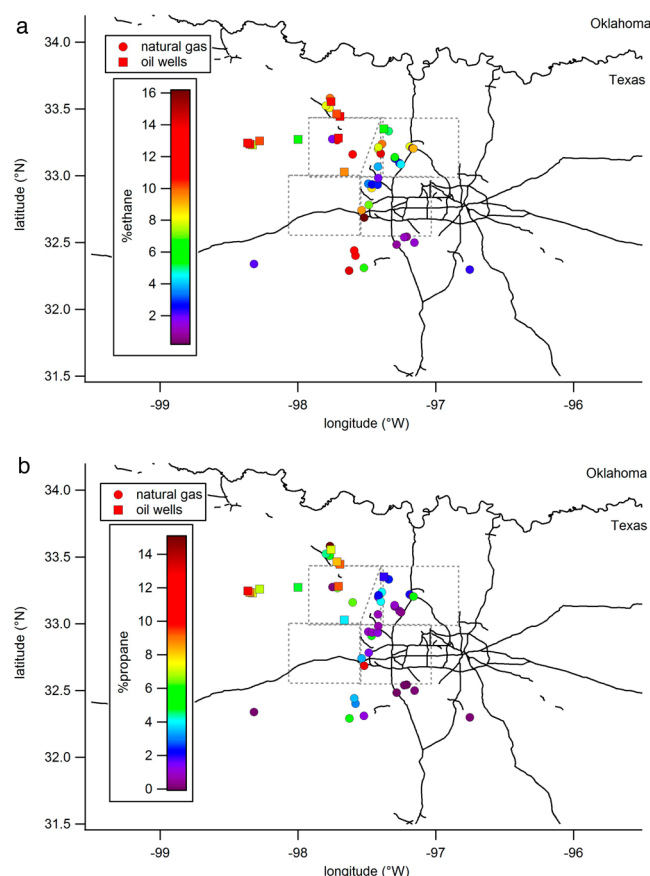
Table 3. Background-Corrected Stable Isotope Ratios and C_3/C_1 , $n-C_4/C_1$, and $n-C_5/C_1$ Ratios for Various CH_4 Sources in the Barnett Region (See Text)^a

sample type	mean $\delta^{13}C-CH_4$	range $\delta^{13}C-CH_4$	mean $\delta D-CH_4$	range $\delta D-CH_4$	mean C_3/C_1	range C_3/C_1	mean $n-C_4/C_1$	range $n-C_4/C_1$	mean $n-C_5/C_1$	range $n-C_5/C_1$
cattle	-52.1 ± 6.0	-58.1 to -42.3	-224 ± 57	-268 to -118	—	—	—	—	—	—
landfills	-51.3 ± 3.3	-56.1 to -47.2	-205 ± 44	-269 to -147	—	—	—	—	—	—
natural gas well pads	-46.6 ± 4.1	-56.2 to -41.2	-150 ± 29	-232 to -89	4.97 ± 7.49	-0.05 to 34.52	1.49 ± 2.82	-0.03 to 14.51	0.64 ± 1.23	-0.02 to 6.45
transmission compressor stations	-46.7 ± 2.6	-52.4 to -43.4	-151 ± 12	-172 to -131	6.03 ± 13.59	0.11 to 44.25	3.74 to 10.43	0.00 to 33.38	1.34 ± 3.79	0.00 to 12.10
distribution systems	-46.9 ± 5.9	-55.5 to -42.2	-138 ± 23	-172 to -119	0.63 ± 0.71	0.05 to 1.57	0.16 ± 0.23	-0.02 to 0.48	-0.01 ± 0.15	-0.01 to 0.15
conventional oil wells	-48.4 ± 3.8	-53.1 to -44.2	-177 ± 19	-208 to -161	9.76 ± 4.56	2.13 to 19.66	3.38 ± 2.10	0.64 to 8.71	1.23 ± 0.83	0.29 to 3.30

^aMean is \pm standard deviation (SD). C_2/C_1 ratios are shown in Table 4. — = not applicable.

Table 4. Background Corrected Data from Natural Gas Production Sites from the Current Study and Two Previous Studies

	<i>n</i>	min C_2/C_1 (% by vol)	max C_2/C_1 (% by vol)	median C_2/C_1 (% by vol)	mean C_2/C_1 (% by vol)	standard deviation C_2/C_1 (% by vol)
this study	30	0.3	30.7	7.5	8.3	7.1
ERG ³⁹	102	1.0	13.4	2.1	5.0	4.3
Zumberge et al. ³⁸	129	0.7	13.1	2.1	4.5	1.2

**Figure 5.** Map of (a) % ethane and (b) % propane in natural gas and oil wells in the Barnett region. Dotted lines are the “core” Barnett Shale counties.

samples and a broader geographic sampling area. The two previous studies also made measurements at the well pad, either from the wellhead³⁸ or from condensate tanks.³⁹ Our samples were collected downwind of well pads where $[CH_4]$ was elevated by at least 50 ppb and, therefore, may represent a higher proportion of tank flashing events than previous studies, which may explain the higher content of non- CH_4 hydrocarbons.

Our previous work applying isotopic measurements to emissions of CH_4 in urban southern California indicated that $\delta D-CH_4$ was a better tracer of CH_4 sources in top-down measurements than $\delta^{13}C-CH_4$, although we found similar values for δD and $\delta^{13}C$ of CH_4 from different sources in both California and Texas.⁷ In the Barnett region, this also appears to be the case (Figures 2 and 3), although we do not have top-down measurements of $\delta D-CH_4$ in the Barnett. There is a larger variation in $\delta D-CH_4$ versus $\delta^{13}C-CH_4$ among different types of CH_4 , and all of the measured sources have $\delta D-CH_4$ ratios distinct from background air ($\delta D = -114\text{‰}$). On the other hand, some thermogenic CH_4 sources in the Barnett have $\delta^{13}C$ ratios (Table 1 and 3) similar to background air ($\delta^{13}C = -47.9\text{‰}$) and thus are hard to distinguish from background signatures. Importantly, δD can distinguish between CH_4 released from shale gas and conventional oil wells (Figure 3), which may be particularly useful in the Barnett (see further discussion below). Our work indicates that future top-down studies attempting to identify CH_4 sources may benefit from the measurement of $\delta D-CH_4$.

Integrating Source Indicators into a Bottom-up CH_4 Inventory. We used the bottom-up inventory developed in the Barnett Coordinated Campaign,⁴⁰ which includes a range of possible estimates for CH_4 sources along with our isotopic and alkane composition data (derived from ratio plots for individual sources) to compare with the composition of well-mixed air measured in top-down studies (Table 5). The contribution of

Table 5. Bottom-up Inventory of CH₄ Sources in the Barnett Shale Region (Lyon et al.⁴⁰) and Source Signatures for Each Source (Tables 1 and 2)^a

	CH ₄ flux (kg CH ₄ /h)	δ ¹³ C-CH ₄ (‰)	δD-CH ₄ (‰)	C ₂ H ₆ /CH ₄ (%)	C ₃ H ₈ /CH ₄ (%)
active gas well pads	16 400	−45.4	−148	6.0	2.0
active oil well pads	1800	−49.2	−170	13.0	6.0
inactive wells	630	−45.4	−148	6.0	2.0
well completions	150	−45.4	−148	6.0	2.0
gathering compressors	18 700	−45.4	−148	6.0	2.0
gathering pipelines	940	−45.4	−148	6.0	2.0
processing plants	5500	−45.4	−148	6.0	2.0
transmission and storage compressors	1600	−45.8	−145	7.0	3.0
transmission pipelines	230	−45.8	−145	7.0	3.0
residential and commercial end users	160	−44.6	−133	6.0	2.0
local distribution	680	−44.6	−133	6.0	2.0
natural gas vehicles	14	−44.6	−133	6.0	2.0
other industrial sources	60	−45.4	−148	6.0	2.0
vehicles (gas and diesel) ¹⁰	150	−30.3	−122	0.0	0.0
landfills	11 300	−54.8	−260	0.0	0.0
livestock	11 900	−56.3	−283	0.0	0.0
wastewater treatment ¹⁰	760	−46.7	−298	0.0	0.0
geological seepage	1100	−45.4	−148	6.0	0.3
total emissions	72 300	−48.9	−190	4.2	1.4

^aLower-bound and upper-bound estimates are also included in the text and Table S1 of the Supporting Information. More detailed calculations, including bottom-up fluxes of C₂H₆, are shown in Table S1, Supporting Information. Ratios of *n*-butane and *n*-pentane to methane were not included due to generally low statistical significance for these ratios for most sources (Table 2).

each CH₄ source to total emissions was multiplied by each alkane or isotopic ratio endmember. We also used literature values for the isotopic composition of CH₄ emitted from wastewater treatment plants and gasoline-powered vehicles, not measured in the current study.⁷ Geological seepage and abandoned wells were not measured, so we assumed the same composition as active natural gas wells.^{41,42} We also assumed that natural gas at gathering and processing plants was identical to wellhead gas, while storage facilities had the same composition as transmission compressor stations (Table 5). Natural gas vehicles were assumed to emit CH₄ with the same composition as distribution gas.

Integrating the bottom-up inventory with our source apportionment data provides an overall isotopic and alkane ratio for emissions from the Barnett Shale/Fort Worth region (Table 5). We also used the C₂/C₁ ratio from the bottom-up inventory to calculate a flux of C₂H₆ from the region (overall C₂/C₁ multiplied by the CH₄ emission for each scenario: median, low end, and high end) of 5.7×10^3 kg C₂H₆ h^{−1} (5.3 – 6.2×10^3 kg C₂H₆ h^{−1}) (Supporting Information). This is in good agreement with top-down measurements of C₂H₆ emissions in the region made during the Barnett Coordinated Campaign ($6.6 \pm 0.2 \times 10^3$ kg C₂H₆ h^{−1}).⁴³

For further comparison, we also substituted our background-corrected average C₂/C₁ ratio (Table 4) into the bottom-up inventory, along with values of C₂/C₁ from previous studies (Table S1, Supporting Information).^{38,39} Use of our background-corrected (rather than ratio plot-derived) C₂/C₁ ratio yields a flux of C₂H₆ of 7.6×10^3 kg h^{−1}, with low and high end estimates of 7.1×10^3 and 8.3×10^3 kg h^{−1}. The two previous studies both found an average C₂/C₁ ratio from natural gas production that was lower than our average value (Table 4) and therefore lead to average C₂H₆ fluxes that are lower than our estimates. Using data from refs 28 and 29 for natural gas production sites yield a C₂H₆ flux of 4.4×10^3 kg C₂H₆ h^{−1} (4.2 – 4.8×10^3 kg C₂H₆ h^{−1}) and 4.9×10^3 kg C₂H₆ h^{−1} (4.6 – 5.3×10^3 kg C₂H₆ h^{−1}), respectively. While these fluxes are similar to that measured in the Barnett top-down study,⁴³ the bottom-up inventory estimates a smaller contribution of oil and gas to total CH₄ emissions (52–78%) than the top-down study (71–85%).^{40,43} The wide range of gas composition and δ¹³C-CH₄ observed in the Barnett region is problematic for top-down source apportionment using a simple mixing model, although utilizing the full range of C₂/C₁ values in top-down approaches can be successful.⁴³ Emissions from production sites are spatially and temporally heterogeneous,²⁵ and our work shows that they may be compositionally heterogeneous as well (Figure 5a,b). δD-CH₄ may be more useful for simple mixing models in top-down source apportionment, particularly since δD may distinguish between various fossil fuel CH₄ sources (Figures 2 and 3).

We observed emissions from conventional oil wells that were enriched in C₂/C₁ relative to natural gas sources (13% versus 6%) (Tables 2–4; Figure 5a). One potential pitfall of using C₂/C₁ as the sole source indicator for top-down studies is that observations of elevated C₂/C₁ in oil production regions could lead to overestimation of oil and gas emissions if C₂/C₁ values used for source apportionment are based primarily on natural gas wells. Although the bottom-up inventory (Table 5) is in general agreement with the top-down C₂H₆ flux presented in ref 43, the lower average C₂/C₁ used in ref 43 may explain the generally higher proportion of total CH₄ emissions attributed to oil and gas activities by the top-down study⁴³ versus the bottom-up inventory⁴⁰. The estimate of oil well CH₄ emissions in ref 40 is less than 3% of total emissions, suggesting that oil well emissions have a minor impact on source apportionment, but these estimates are highly uncertain since underlying data were based primarily on fluxes measured from natural gas wells (96% of flux measurements).^{44–47} Future source apportionment efforts in the Barnett region may benefit from a spatially explicit inventory of CH₄ and C₂H₆ that includes emissions from oil wells.

Comparison to Other Regions. Our work and other research conducted as part of the Barnett Coordinated Campaign indicates that the Fort Worth–Barnett shale region (part of the United States' fourth largest metropolitan area) has a larger proportion of biological CH₄ emissions than other cities, despite the large amount of natural gas production in this region. Observations of δ¹³C, δD, and alkane ratios in Los Angeles, CA showed that the dominant CH₄ source was likely fugitive emissions of thermogenic CH₄, perhaps from natural gas infrastructure,^{7,19,20} whereas the bottom-up inventory suggests a mixture of biological and thermogenic CH₄ sources in the Barnett region (Table 5).⁴⁰ In Boston, natural gas infrastructure is the dominant CH₄ source.⁸ Denver, home to a large oil and gas production industry, has 22–24% of CH₄ from

nonoil and gas sources, mainly cattle and waste industries,²⁴ compared to 33% in the Barnett. Other large urban areas, including Beijing,⁴⁸ London,^{18,49,50} and St. Petersburg,⁵¹ have a mixture of biological and fossil fuel CH₄ sources similar to the Fort Worth region. Unlike these cities, which lack oil and gas production, the contribution of natural gas distribution systems to CH₄ emissions in Fort Worth is small (~1%) (Table 5). Overall, our work indicates that the Barnett region represents a complex mixture of urban, agricultural, and fossil fuel CH₄ sources, with challenging implications for source apportionment of CH₄ emissions.

■ ASSOCIATED CONTENT

■ Supporting Information

Raw data and Table S1. The Supporting Information is available free of charge on the ACS Publications website at DOI: 10.1021/acs.est.5b00057.

■ AUTHOR INFORMATION

Corresponding Author

*E-mail: amy.townsend-small@uc.edu; phone: 513-556-3762; fax: 513-556-6931.

Notes

The authors declare no competing financial interest.

■ ACKNOWLEDGMENTS

We thank Ramón Alvarez, Claire Botner, Nigel Clark, April Covington, Steve Edburg, Tom Ferrara, Morgan Gallagher, Bob Harriss, Touché Howard, Rob Jackson, Kristine Jimenez, Brian Lamb, Gloria Liu, Brent Love, Chris Rella, Robert Talbot, and Tracy Tsai for their assistance with this project. Funding was provided by the Environmental Defense Fund (EDF) and the National Science Foundation (Award No. 1229114). Funding for EDF's methane research series, including this work, is provided by Fiona and Stan Druckenmiller, Heising-Simons Foundation, Bill and Susan Oberndorf, Betsy and Sam Reeves, Robertson Foundation, Alfred P. Sloan Foundation, TomKat Charitable Trust, and the Walton Family Foundation.

■ REFERENCES

- (1) Myhre, G.; Shindell, D.; Bréon, F.-M.; Collins, W.; Fuglestedt, J.; Huang, J.; Koch, D.; Lamarque, J. F.; Lee, D.; Mendoza, B.; et al. Anthropogenic and Natural Radiative Forcing. In *Climate Change 2013: The Physical Science Basis. Contribution of Working Group I to the Fifth Assessment Report of the Intergovernmental Panel on Climate Change*; Stocker, T. F.; Qin, D.; Plattner, G.-K.; Tignor, M.; Allen, S. K.; Boschung, J.; Nauels, A.; Xia, Y.; Bex, V.; Midgley, P. M., Eds.; Cambridge University Press: New York, 2013.
- (2) Kirschke, S.; Bosquet, P.; Ciais, P.; Saunoy, M.; Canadell, J. G.; Dlugokencky, E. J.; Bergamaschi, P.; Bergmann, D.; Blake, D. R.; Bruhwiler, L.; et al. Three decades of global methane sources and sinks. *Nat. Geosci.* **2013**, *6*, 813–823 DOI: 10.1038/ngeo1955.
- (3) Schwietzke, S.; Griffin, W. M.; Matthews, H. S.; Bruhwiler, L. M. P. Global bottom-up fossil fuel fugitive methane and ethane emissions inventory for atmospheric modeling. *ACS Sustainable Chem. Eng.* **2014**, *2*, 1992–2001 DOI: 10.1021/sc500163h.
- (4) Schwietzke, S.; Griffin, W. M.; Matthews, H. S.; Bruhwiler, L. M. P. Natural gas fugitive emissions rates constrained by global atmospheric methane and ethane. *Environ. Sci. Technol.* **2014**, *48*, 7714–7722 DOI: 10.1021/es501204c.
- (5) United States Environmental Protection Agency (USEPA). *Inventory of U.S. Greenhouse Gas Emissions and Sinks: 1990–2012*; EPA 430-R-14-003; USEPA: Washington, DC, 2014; <http://www.epa.gov/climatechange/emissions/usinventoryreport.html>.
- (6) Leifer, I.; Culling, D.; Schneising, O.; Farrell, P.; Buchwitz, M.; Burrows, J. P. Transcontinental methane measurements: Part 2. Mobile surface investigation of fossil fuel industrial fugitive emissions. *Atmos. Environ.* **2013**, *74*, 432–441 DOI: 10.1016/j.atmosenv.2013.03.018.
- (7) Townsend-Small, A.; Tyler, S. C.; Pataki, D. E.; Xu, X.; Christensen, L. E. Isotopic measurements of atmospheric methane in Los Angeles, California, USA: Influence of “fugitive” fossil fuel emissions. *J. Geophys. Res.* **2012**, *117* (D7), D07308.
- (8) McKain, K.; Down, A.; Raciti, S. M.; Budney, J.; Hutyra, L. R.; Floerchinger, C.; Herndon, S. C.; Nehrkorn, T.; Zahniser, M. S.; Jackson, R. B.; et al. Methane emissions from natural gas infrastructure and use in the urban region of Boston, Massachusetts. *Proc. Nat. Acad. Sci.* **2015**, *112*, 1941–1946 DOI: 10.1073/pnas.1416261112.
- (9) Wigley, T. M. L. Coal to gas: The influence of methane leakage. *Clim. Change* **2011**, *108*, 601–608.
- (10) Pacyna, E. G.; Pacyna, J. M.; Steenhuisen, F.; Wilson, S. Global anthropogenic mercury emission inventory for 2000. *Atmos. Environ.* **2006**, *40*, 4048–4063 DOI: 10.1016/j.atmosenv.2006.03.041.
- (11) Brandt, A. R.; Heath, G. A.; Kort, E. A.; O'Sullivan, F.; Pétron, G.; Jordaan, S. M.; Tans, P.; Wilcox, J.; Gopstein, A. M.; Arent, D.; et al. Methane leaks from North American natural gas systems. *Science* **2014**, *343*, 733–735 DOI: 10.1126/science.1247045.
- (12) Lamb, B. K.; Edburg, S. L.; Ferrara, T. W.; Howard, T.; Harrison, M. R.; Kolb, C. E.; Townsend-Small, A.; Dyck, W.; Possolo, A.; Whetstone, J. R. Direct measurements show decreasing methane emissions from natural gas local distribution systems in the United States. *Environ. Sci. Technol.* **2015**, DOI: 10.1021/es201405116p.
- (13) Mitchell, A. L.; Tkacik, D. S.; Roscioli, J. R.; Herndon, S. C.; Yacovitch, T. I.; Martinez, D. M.; Vaughn, T. L.; Sullivan, M. R.; Floerchinger, C.; et al. Measurements of methane emissions from natural gas gathering facilities and processing plants: Measurement results. *Environ. Sci. Technol.* **2015**, DOI: 10.1021/es5052809.
- (14) Subramanian, R.; Williams, L. R.; Vaughn, T. L.; Zimmerle, D.; Roscioli, J. R.; Herndon, S. C.; Yacovitch, T. I.; Floerchinger, C.; Tkacik, D. S.; Mitchell, A. L.; et al. Methane emissions from natural gas compressor stations in the transmission and storage sector: Measurements and comparisons with the EPA greenhouse gas reporting program protocol. *Environ. Sci. Technol.* **2015**, DOI: 10.1021/es5060258.
- (15) Wunch, D.; Wennberg, P. O.; Toon, G. C.; Keppel-Aleks, G.; Yavin, Y. G. Emissions of greenhouse gases from a North American megacity. *Geophys. Res. Lett.* **2009**, *36*, L15810 DOI: 10.1029/2009GL039825.
- (16) Hsu, Y. K.; VanCuren, T.; Park, S.; Jakober, C.; Herner, J.; FitzGibbon, M.; Blake, D. R.; Parrish, D. D. Methane emissions inventory verification in southern California. *Atmos. Environ.* **2010**, *44*, 1–7 DOI: 10.1016/j.atmosenv.2009.10.002.
- (17) Miller, S. M.; Wofsy, S. C.; Michalak, A. M.; Kort, E. A.; Andrews, A. E.; Biraud, S. C.; Dlugokencky, E. J.; Eluszkiewicz, J.; Fischer, M. L.; Janssens-Maenhout, G.; et al. Anthropogenic emissions of methane in the United States. *Proc. Natl. Acad. Sci. U.S.A.* **2013**, DOI: 10.1073/pnas.1314392110.
- (18) Fisher, R.; Lowry, D.; Wilkin, O.; Sriskantharajah, S.; Nisbet, E. G. High-precision, automated stable isotope analysis of atmospheric methane and carbon dioxide using continuous-flow isotope-ratio mass spectrometry. *Rapid Commun. Mass Spectrom.* **2006**, *20*, 200–208 DOI: 10.1002/rcm.2300.
- (19) Peischl, J.; Ryerson, T. B.; Brioude, J.; Aikin, K. C.; Andrews, A. E.; Atlas, E.; Blake, D.; Daube, B. C.; de Gouw, J. A.; Dlugokencky, E.; et al. Quantifying sources of methane using light alkanes in the Los Angeles basin, California. *J. Geophys. Res.* **2013**, *118*, 4974–4990 DOI: 10.1002/jgrd.50413.
- (20) Wennberg, P. O.; Mui, W.; Wunch, D.; Kort, E. A.; Blake, D. R.; Atlas, E. L.; Santoni, G. W.; Wofsy, S. C.; Diskin, G. S.; Jeong, S.; et al. On the sources of methane to the Los Angeles atmosphere. *Environ. Sci. Technol.* **2012**, *46*, 9282–9289 DOI: 10.1021/es301138y.
- (21) Katzenstein, A. S.; Doeze, L. A.; Simpson, I. J.; Blake, D. R.; Rowland, F. S. Extensive regional atmospheric hydrocarbon pollution

in the southwestern United States. *Proc. Natl. Acad. Sci. U.S.A.* **2003**, *100*, 11975–11979 DOI: 10.1073/pnas.1635258100.

(22) Karion, A.; Sweeney, C.; Pétron, G.; Frost, G.; Hardesty, R. M.; Kofler, J.; Miller, B. R.; Newberger, T.; Wolter, S.; Banta, R.; et al. Methane emissions estimate from airborne measurements over a western United States natural gas field. *Geophys. Res. Lett.* **2013**, *40*, 4393–4397 DOI: 10.1002/grl.50811.

(23) Pétron, G.; Frost, G.; Miller, B. R.; Hirsch, A. I.; Montzka, S. A.; Karion, A.; Trainer, M.; Sweeney, C.; Andrews, A. E.; Miller, L.; et al. Hydrocarbon emissions characterization in the Colorado Front Range: A pilot study. *J. Geophys. Res.* **2012**, *117*, D04304 DOI: 10.1029/2011JD016360.

(24) Pétron, G.; Karion, A.; Sweeney, C.; Miller, B. R.; Montzka, S. A.; Frost, G. J.; Trainer, M.; Tans, P.; Andrews, A.; Kofler, J.; et al. A new look at methane and nonmethane hydrocarbon emissions from oil and natural gas operations in the Colorado Denver-Julesburg Basin. *J. Geophys. Res.* **2014**, *119*, 6386–6852 DOI: 10.1002/2013JD021272.

(25) Allen, D. T.; Torres, V. M.; Thomas, J.; Sullivan, D. W.; Harrison, M.; Hendler, A.; Herndon, S. C.; Kolb, C. E.; Fraser, M. P.; Hill, A. D.; et al. Measurements of methane emissions at natural gas production sites in the United States. *Proc. Natl. Acad. Sci. U.S.A.* **2013**, DOI: 10.1073/pnas.1304880110.

(26) Harriss, R. S.; Alvarez, R.; Lyon, D.; Hamburg, S.; Nelson, D.; Zavala-Araiza, D. Using multi-scale measurements to improve methane emissions estimates from oil and gas operations in the Barnett Shale, Texas: Campaign Summary. *Environ. Sci. Technol.*, DOI: 10.1021/acs.est.5b02305.

(27) Simpson, I. J.; Blake, N. J.; Barletta, B.; Diskin, G. S.; Fuelberg, H. E.; Gorham, K.; Huey, L. G.; Meinardi, S.; Rowland, F. S.; Vay, S. A.; et al. Characterization of trace gases measured over Alberta oil sands mining operations: 76 speciated C₂–C₁₀ volatile organic compounds (VOCs), CO₂, CH₄, NO, NO₂, NO_y, O₃, and SO₂. *Atmos. Chem. Phys.* **2010**, *10*, 11931–11954 DOI: 10.519/acp-10-11931-2010.

(28) Crosson, E. R. A cavity ring-down analyzer for measuring atmospheric levels of methane, carbon dioxide, and water vapor. *Appl. Phys. B: Laser Opt.* **2008**, *92*, 403–408 DOI: 10.1007/s00340-008-3135-y.

(29) Colman, J. J.; Swanson, A. L.; Meinardi, S.; Sive, B. C.; Blake, D. R.; Rowland, F. S. Description of the analysis of a wide range of volatile organic compounds in whole air samples collected during PEM-Tropics A and B. *Anal. Chem.* **2001**, *73*, 3723–3731.

(30) Yarnes, C. $\delta^{13}\text{C}$ and $\delta^2\text{H}$ measurement of methane from ecological and geological sources by gas chromatography/combustion/pyrolysis isotope-ratio mass spectrometry. *Rapid Commun. Mass Spectrom.* **2013**, *27*, 1036–1044 DOI: 10.1002/rcm.6549.

(31) Keeling, C. D. The concentration and isotopic abundances of atmospheric carbon dioxide in rural areas. *Geochim. Cosmochim. Acta* **1958**, *13*, 322–334 DOI: 10.1016/0016-7037(58)90033-4.

(32) Keeling, C. D. The concentration and isotopic abundances of carbon dioxide in rural and marine air. *Geochim. Cosmochim. Acta* **1961**, *24*, 277–298 DOI: 10.1016/0016-7037(61)90023-0.

(33) Pataki, D. E.; Ehleringer, J. R.; Flanagan, L. B.; Yakir, D.; Bowling, D. R.; Still, C. J.; Buchmann, N.; Kaplan, J. O.; Berry, J. A. The application and interpretation of Keeling plots in terrestrial carbon cycle research. *Global Biogeochem. Cycles* **2003**, *17*, 1022 DOI: 10.1029/2001GB001850.

(34) White, J. W. C.; Vaughn, B. H. *Stable isotopic composition of atmospheric methane (^{13}C) from the NOAA ESRL Carbon Cycle Cooperative Global Air Sampling Network, 1998–2011*; version: 2013-04-05; University of Colorado, Institute of Arctic and Alpine Research (INSTAAR): Boulder, 2011.

(35) Dlugokencky, E. J.; Lang, P. M.; Crotwell, A. M.; Masarie, K. A.; Crotwell, M. J. Atmospheric methane dry air mole fractions from the NOAA ESRL Carbon Cycle Cooperative Global Air Sampling Network, 1983–2013; version: 2014-6-24; 2014. Available at ftp://aftp.cmdl.noaa.gov/data/trace_gases/ch4/flask/surface/.

(36) Whiticar, M. J. Carbon and hydrogen isotope systematics of bacterial formation and oxidation of methane. *Chem. Geol.* **1999**, *161*, 291–314 DOI: 10.1016/S0009-2541(99)00092-3.

(37) Whiticar, M. J.; Schaefer, H. Constraining past global tropospheric methane budgets with carbon and hydrogen isotope ratios in ice. *Philos. Trans. R. Soc. A* **2007**, *365*, 1793–1828 DOI: 10.1098/rsta.2007.2048.

(38) Zumberge, J.; Ferworn, K.; Brown, S. Isotopic reversal ('rollover') in shale gases produced from the Mississippian, Barnett, and Fayetteville formations. *Mar. Pet. Geol.* **2012**, *31*, 43–52.

(39) Eastern Research Group (ERG). *Condensate tank oil and gas activities: Final Report*; Prepared for the Texas Commission on Environmental Quality, Air Quality Division; 2012. Available at https://www.tceq.texas.gov/assets/public/implementation/air/am/contracts/reports/ei/5821199776FY1211-20121031-ergi-condensate_tank.pdf.

(40) Lyon, D.; Zavala-Araiza, D.; Alvarez, R.; Harriss, R.; Palacios, V.; Lan, X.; Lavoie, T.; Mitchell, A.; Yacovitch, T.; Hamburg, S. Constructing a spatially-resolved methane emission inventory for the Barnett Shale region. *Environ. Sci. Technol.*, DOI: 10.1021/es506359c.

(41) Etiope, G.; Drobniak, A.; Schimmelmann, A. Natural seepage of shale gas and the origin of "eternal flames" in the Northern Appalachian Basin, USA. *Mar. Petrol. Geol.* **2013**, *43*, 178–186 DOI: 10.1016/j.marpetgeo.2013.02.009.

(42) Kang, M.; Kanno, C. M.; Reid, M. C.; Zhang, X.; Mauzerall, D. L.; Celia, M. A.; Chen, Y.; Onstott, T. C. Direct measurements of methane emissions from abandoned oil and gas wells in Pennsylvania. *Proc. Natl. Acad. Sci. U.S.A.* **2014**, DOI: 10.1073/pnas.1408315111.

(43) Smith, M. L.; Kort, E. A.; Karion, A.; Sweeney, C.; Herndon, S.; Newberger, T.; Wolter, S.; Yacovitch, T. Airborne ethane observations in the Barnett shale: Quantification of ethane flux and attribution of methane emissions. *Environ. Sci. Technol.*, DOI: 10.1021/acs.est.5b00219.

(44) Yacovitch, T. I.; Herndon, S. C.; Pétron, G.; Kofler, J.; Lyon, D.; Alvarez, R.; Zahniser, M. S.; Kolb, C. E. Mobile laboratory observations of methane emissions in the Barnett Shale region. *Environ. Sci. Technol.* **2015**, DOI: 10.1021/es506352j.

(45) Zavala-Araiza, D.; Lyon, D.; Alvarez, R. A.; Palacios, V.; Harriss, R.; Lan, X.; Talbot, R.; Hamburg, S. P. Toward a functional definition of methane super-emitters: Application to natural gas production sites. *Environ. Sci. Technol.*, DOI: 10.1021/es5b00133.

(46) Rella, C. W.; Tsai, T. R.; Botkin, C. G.; Crosson, E. R.; Steele, D. Measuring emissions from oil and natural gas well pads using the mobile flux plane technique. *Environ. Sci. Technol.* **2015**, DOI: 10.1021/acs.est.5b00099.

(47) Lan, X.; Talbot, R.; Laine, P.; Torres, A. Characterizing fugitive methane emissions in the Barnett using a mobile laboratory. *Environ. Sci. Technol.*, DOI: 10.1021/es5063055.

(48) Su, F.; Shao, M.; Cai, X.; Zeng, L.; Zhu, T. Estimates of methane emissions in Beijing using a backward trajectory inversion model. *Chem. Speciation Bioavailability* **2003**, *14*, 43–48.

(49) O'Shea, S. J.; Allen, G.; Fleming, Z. L.; Bauguitte, S. J. B.; Percival, C. J.; Gallagher, M. W.; Lee, J.; Helfter, C.; Nemitz, E. Area fluxes of carbon dioxide, methane, and carbon monoxide derived from airborne measurements around Greater London: A case study during summer 2012. *J. Geophys. Res.* **2014**, *119*, 4940–4952 DOI: 10.1002/2013JD021269.

(50) Lowry, D.; Holmes, C. W.; Rata, N. D.; O'Brien, P.; Nisbet, E. G. London methane emissions: Use of diurnal changes in concentration and $\delta^{13}\text{C}$ to identify urban sources and verify inventories. *J. Geophys. Res.* **2001**, *106*, 7427–7448 DOI: 10.1029/2000JD900601.

(51) Zinchenko, A. V.; Paramonova, N. N.; Privalov, V. I.; Reshetnikov, A. I. Estimation of methane emissions in the St. Petersburg, Russia, region: An atmospheric boundary layer budget approach. *J. Geophys. Res.* **2002**, *107*, 4416 DOI: 10.1029/2001JD001369.